AD-A138 585 ON THE LIMITING ELECTRODE POTENTIAL IN CAVITIES AND ITS ROLE IN DECIDING B..(U) PENNSYLVANIA STATE UNIV UNIVERSITY PARK DEPT OF MATERIALS SCI.. H W PICKERING 1/1

UNCLASSIFIED FEB 84 N00014-81-K-0025 F/G 7/4 NL

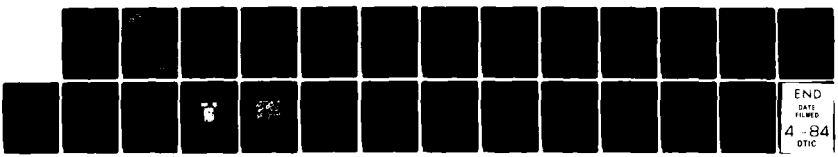

END
DATE FILMED
4-84
DTIC

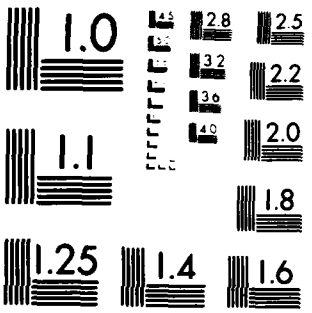

(12

COLLEGE OF EARTH AND MINERAL SCIENCES

DEPARTMENT OF MATERIALS SCIENCE

METALLURGY PROGRAM

TECHNICAL REPORT

February 1984

OFFICE OF NAVAL RESEARCH

Contract No. N000-14-81-K-0025

ON THE LIMITING ELECTRODE POTENTIAL IN CAVITIES AND ITS ROLE IN DECIDING BETWEEN SCC AND HC IN METALS

H. W. Pickering

Department of Materials Science and Engineering
The Pennsylvania State University
University Park, Pennsylvania 16802

The Pennsylvania State University

University Park, Pennsylvania

THE PENNSYLVANIA STATE UNIVERSITY

College of Earth and Mineral Sciences

UNDERGRADUATE PROGRAMS OF STUDY

Ceramic Science and Engineering, Earth Sciences, Fuel Science, Geography, Geosciences, Metallurgy, Meteorology, Mineral Economics, Mining Engineering, Petroleum and Natural Gas Engineering, and Polymer Science.

GRADUATE PROGRAMS AND FIELDS OF RESEARCH

Ceramic Science, Fuel Science, Geochemistry and Mineralogy, Geography, Geology, Geophysics, Metallurgy, Meteorology, Mineral Economics, Mineral Processing, Mining Engineering, Petroleum and Natural Gas Engineering, and Polymer Science.

UNIVERSITY-WIDE INTERDISCIPLINARY GRADUATE PROGRAMS INVOLVING E&MS FACULTY AND STUDENTS

Earth Sciences, Ecology, Environmental Pollution Control Engineering, Mineral Engineering Management, Operations Research, Regional Planning, and Solid State Science.

ASSOCIATE DEGREE PROGRAMS

Metallurgical Engineering Technology and Mining Technology.

INTERDISCIPLINARY RESEARCH GROUPS WITHIN THE COLLEGE

Coal Research Section, Mineral Conservation Section, Ore Deposits Research Section, and Mining and Mineral Resources Research Institute.

ANALYTICAL AND STRUCTURE STUDIES

Classical chemical analysis of metals and silicate and carbonate rocks; X-ray crystallography; electron microscopy and diffraction; electron microprobe analysis; atomic absorption analysis; spectrochemical analysis.

U.Ed. 9-725

ON THE LIMITING ELECTRODE POTENTIAL IN CAVITIES AND ITS ROLE IN DECIDING BETWEEN SCC AND HC IN METALS

BY

H. W. Pickering

Tecnhical Report

to

Office of Naval Research

Contract No. N000-14-81-K-0025

February 1984

A-1

Introduction

In an aqueous solution there are defined regions of electrode potential for the hydrogen evolution and anodic metal dissolution reactions. These two regions of potential differ with respect to each other depending on the metal and solution composition. In those cases where the metal does not already contain hydrogen, the former (hydrogen evolution) is necessary to generate hydrogen which can then cause hydrogen cracking (HC), and the metal dissolution reaction is necessary to cause anodic stress corrosion cracking (SCC). It follows that HC and SCC occur in specific potential regions which may or may not overlap. If overlap occurs, both modes of cracking are possible in a specific alloy/electrolyte system for either anodic or cathodic polarization. If overlap does not occur, then only one or the other mode of cracking can occur depending on the electrode potential: HC at potentials less noble than the H equilibrium potential and SCC at potentials more noble than the metal equilibrium potential. Although this is an easily accepted concept it can not be readily applied, mainly because of a lack of specific information on the electrochemical conditions within a crack, in particular at the crack tip where crack propagation occurs. It is the purpose of this paper to more fully explore the application of this concept to actual metal/solution systems.

For alloys containing base metals the potential regions of anodic metal dissolution and of the hydrogen evolution reaction (h.e.r.) overlap at the alloy surface and therefore, also along part or all of the fracture or cavity surface. Thus, for base-metal alloys this concept has no utility for distinguishing between HC and SCC for either anodic or cathodic polarization. For all noble metal alloys in non complexing solutions, on the other hand, no overlap occurs at the alloy surface. To distinguish between HC and SCC however, it is necessary to know if overlap is avoided everywhere in the crack. Although this has been an intractable problem, two rather recent developments appear to provide the necessary information to answer the overlap question. The first is the combined progress in mathematically modeling and measurement of the electrochemical conditions in cavities and cracks. When only soluble reaction products are produced good agreement has been found between calculated and measured electrode potentials (1-4). In addition, the models have been developed from first principles. As a result one can accept with confidence the predicted trends in species concentration, if not the values themselves, as a function of distance x into the cavity. The second is the determination and definition of the limiting potential, E_{LIM}, which can exist in a cavity or crack during anodic or cathodic polarization (3-6). This concept, although new, can also be accepted with confidence since it, too, is developed from first principles and has already some experimental confirmation. Using these developments one finds that is is not necessary to know the actual conditions of electrode potential and solution composition at the crack tip to determine if overlap is avoided everywhere in the crack. This finding is decisive for the goal of this paper which is to determine if for the noble metal alloys only HC can occur during cathodic polarization and only (anodic) SCC during anodic polarization or during open circuit corrosion in the presence of an oxidant (of otherwise hydrogen-free noble metal alloys).

The importance of not needing to know the actual electrode potential at the crack tip is not overstated, since (i) it can vary over a wide range and (ii) its measurement (at the crack tip) is virtually impossible in spite of the considerable progress that has been made in the past decade in the measurement of the local electrode potential in cavities. Direct measurement has shown that the electrode potential in the cavity can differ greatly from that at the outer surface, i.e., by hundreds and even thousands

of mV (1-4, 7-10). This recent success in characterizing the electrode potential in cavities has increased our awareness of just how different the electrode potential (as well as the electrolyte composition) can be in a cavity. It has also become apparent that the measurement technique sometimes disturbs the system and precludes the measurement of the electrode potential in the most constricted regions, e.g., at the crack tip or at the interface of a gas bubble and a cavity surface.

Clearly, an alternative approach to measuring the electrode potential is needed. The one used in this paper and elsewhere (3-6) is to determine from first principles the limiting electrode potential that can exist in a crack for a given metal and use it to obtain an answer on the overlap question. This analysis is straight forward. It leads to the conclusion that (i) there is a limiting potential, E_{LIM}, and (ii) its value varies with solution conditions but never exceeds the equilibrium potential of the thermodynamically most favored reaction of all reactions contributing to the net anodic or cathodic current flowing between the bulk solution and crack tip, i.e. in or out of the crack.

Results and Discussion

The Concept of a Limiting Potential (3,6)

In this section the concept of a limiting potential E_{LIM}, is developed for an oxidation or reduction reaction occurring at the base of a cavity, x = L, the outer surface and side walls of the cavity being inert, e.g., as if covered by a passivating-type film. The change in electrode potential with distance x into the cavity, E(x), can be approximately equated to the IR voltage within the electrolyte which fills the cavity, in which case

$$E(x) = E_{x=0} + IR(x) \qquad (1)$$

where $E_{x=0}$ is the electrode potential at the opening of the cavity, E(x) is the local electrode potential as a function of distance x into the cavity, I is the current flowing between x=0 and x=L with due regard for the current flow direction, and R(x) is the resistance to current flow between x=0 and position x. This treatment assumes that the diffusion current is relatively small. Eq. (1) shows that E(x) shifts in the noble direction for reduction reactions occurring within the cavity corresponding to a reduced overpotential with increasing x, e.g., towards E^{eq}_{H/H^+} for the h.e.r., and in the less noble direction for oxidation reactions, e.g., towards $E^{eq}_{M/M^{z+}}$ for metal dissolution. It also shows that if I or R(x) is large so is the change in E(x). Conversely, I must be finite or IR=0 and $E(x)=E_{x=0}$, i.e., I can be very small if R is very large and still produce a large IR, but even for R the IR product is zero if I goes to zero. This defines the limiting potential, i.e., E_{LIM} corresponds to a zero current-flow condition in or out of the cavity and the value of $E_{x=L}$ lies between $E_{x=0}$ and E_{LIM}. If the reaction occurs also on the side walls of the cavity, e.g., H_2 evolution (insert in Fig. 8), the limiting current condition becomes one of zero-current flow beyond some depth, rather than zero current flow in or out of the cavity. For the example given this would mean that the local current is essentially zero at some depth x and beyond, corresponding to the E_{LIM} condition but the integrated current flowing into the cavity is nevertheless finite and, therefore, the IR term in Eq. (1) is also finite (even though part of the cavity closely approaches or is at the E_{LIM} condition). Thus, for side wall dissolution E_{LIM} can actually be reached, in contrast to the former situation where E_{LIM} can only be

approached. IR can be very large even for small currents flowing in or out of the cavity if R is very large, e.g., due to in-place gas bubbles (1-5).

For a single reaction occurring in the cavity the zero current-flow condition occurs at depths where the reaction is at equilibrium. It also occurs when a second reaction of opposite sign to the primary reaction, occurs at potentials existing in the cavity (but not at the outer surface) but in this case the zero current-flow condition is at the mixed potential of the two reactions occurring in the cavity. Thus, E_{LIM} is either the equilibrium potential of a single reaction or the mixed potential of multiple reactions of mixed sign. A third possibility is that multiple reactions, all of the same sign, occur in the cavity, in which case E_{LIM} is the equilibrium potential of the thermodynamically most favored reaction, e.g., if all of the reactions are oxidation reactions (current flowing out of the cavity) E_{LIM} is the most negative (least noble) equilibrium potential of these reactions, since it, but not the other equilibrium potentials, corresponds to the zero-current condition.

The above-mentioned E_{LIM} potentials are illustrated in Figures 1-3. A single electrochemical reaction in a cavity could be metal dissolution in a pit with the outer surface (x = 0) in the passive region, Fig. 1a, or hydrogen evolution within a crack as well as at the outer surface, Fig. 1b. E_{LIM} for these examples is then the equilibrium potential (for the local composition of electrolyte in the cavities) of the respective reactions, metal dissolution (Fig. 1a) or hydrogen evolution (Fig. 1b). Figure 1a describes the situation when $E_{x=0}$ is established either by an external power supply or by a suitable oxidant undergoing reduction at the outer surface as part of an open circuit corrosion process.

The situation where a secondary electrochemical reaction of opposite sign to that of the primary reaction occurs in a cavity, can readily be demonstrated in laboratory experiments. For example, large IR voltages inside pits in iron, aluminum or stainless steel samples which were anodically polarized well above the h.e.r. equilibrium potential established a potential within the pit in the region of hydrogen evolution (1,10). Similarly, the potential within a crack during electroplating or cathodic protection may lie in the region of anodic dissolution of the metal being plated or protected (2-5). These situations are illustrated in Fig. 2, and show that E_{LIM} is for these situations a mixed potential established by the reactions occurring within the cavity, since it is at the mixed potential that the net current at $E_{x=L}$ available for flow in or out of the cavity is zero.

Open circuit pitting corrosion, where the cathodic reaction occurs entirely on the outer surface, corresponds to the situation within a cavity in Fig. 1a. When some of the cathodic reaction occurs also on the side walls, the current flowing out of the pit is decreased in proportion to that fraction of the cathodic current which occurs within the pit, and the limiting potential, though less likely to be approached, remains $E^{eq}_{M/M^{z+}}$.

Experimental Confirmation of the Existence of a Limiting Potential

Experimental confirmation of the existence and nature of E_{LIM}, although meager in terms of numbers of independent observations, is available in two different forms. There are (i) measurements of the electrode potential as a function of distance into cavities and (ii) observations of secondary reactions occurring within the cavity.

In principle, if one measures the local electrode potential as a function of distance into a crevice the theory of E_{LIM} predicts that at depths corresponding to E_x approaching E_{LIM}, the local current flow in or out of the cavity approaches zero and as such the local electrode potential is only at best a weak function of distance x into the cavity. Thus, a discontinuity in the E(x) function from a strong to weak dependence of E on x may be expected in the vicinity of E_{LIM}. This behavior has been observed for the h.e.r. within a crevice in Fe, Ni and Cu samples, Fig. 4. In crevices in all three metals the local electrode potential in accord with Eq. (1) increases rather sharply (more noble direction) with increasing distance into the crevice and then its dependency on x weakens and E becomes essentially constant at approximately the predicted E_{LIM}, Table 1. The predicted values of E_{LIM} in Table 1 are mixed potentials in the case of Fe and Ni, and an equilibrium potential (for the h.e.r.) in the case of Cu since $E^{eq}_{Cu/Cu^{++}}$ is more noble than that of the h.e.r. For the rather strong cathodic polarization (10 to 100 A m^{-2}) used in these experiments E_{LIM} was approached only when (gas-bubble) constrictions formed in the cavity effectively increasing R, Fig. 5. This, however, was a normal development for all three metals in a matter of minutes or less.

TABLE 1. Experimental confirmation of the existence of E_{LIM} during cathodic polarization of Fe, Ni and Cu samples in strong acid solution (Cu and Ni) or buffered acetic acid/sodium acetate (pH 5) solution (Fe) (2,3).

Metal	i_c A m^{-2}	E_{LIM}(SHE), V model	E_{LIM}(SHE), V probe	Etched	Metal ions in Crevice
Fe	9	-0.3/-0.6	-0.5	yes	yes
Fe	52	-0.3/-0.6	-0.51	yes	yes
Ni	100	0.0/-0.4	-0.23	yes	yes
Cu	100	$\tilde{<}$ 0.0	$\tilde{>}$ -0.2	no	no

The occurrence of additional electrochemical reactions inside cavities is consistent, in general, with a variation of electrode potential between the outside surface and cavity surface. The discovery and identification of certain additional reactions inside cavities can, in turn, be used as a guide to the ranges of electrode potential that exists in the cavity. Thus, when etching was observed at the bottom of crevices in Fe and Ni samples during strong cathodic polarization and their ions were also found in the electrolyte within the cavities (Fig. 6 and Table 1), it was a clear indication that the electrode potentials in the cavities, although not at the outer surface, were in the regions of anodic dissolution of the respective metals. The salient point, however, with regard to the E_{LIM} theory is that for otherwise identical experiments on Cu samples, neither etching of the Cu nor formation of its ions were observed in the crevice, indicative of the presence of a limiting potential and consistent with the above interpretation of E_{LIM}, i.e. since Cu is a noble metal overlap of its anodic dissolution potential range and that of the h.e.r. could only occur for rather extreme conditions of solution composition. Thus, one can expect (see below for a proof) that $E_{LIM} = E^{eq}_{H/H^+} < E^{eq}_{Cu/Cu^{++}}$ in the

cavity as well as on the outer surface, i.e., the electrode potential everywhere in the cavity is reducing with respect to copper, consistent with the nature of E_{LIM} given above and no copper dissolution, therefore, occurs.

Use of E_{LIM} for Deciding Between HC and SCC

Let us consider a noble-metal alloy/strong acid system, e.g., Cu-Au alloy in dilute $HClO_4$. In this case the standard potential of the least noble metal of the alloy ($E^{o}_{Cu/6u^{++}} = 0.34V$) is more noble than that of the hydrogen evolution reaction ($E_{H/H^{+}} = 0.0V$). Overlap of the potential regions of copper dissolution and hydrogen evolution could only occur for rather extreme conditions of solution composition in metal ions and/or hydrogen ions. Nevertheless, one must know both the trend and magnitude within a cavity or crack of the concentrations of the relevant ionic species in the electrolyte, in order to determine the equilibrium potentials and E_{LIM} at the crack tip.

Using the generalized flux equations for concentration and potential driving forces, the concentration profiles in the cavity at steady state are shown in Figs. 7 and 8 for anodic and cathodic polarization for the Cu-Au alloy, respectively. For anodic polarization (Fig. 7), the pH and the Cu^{++} ion concentration increase with increasing distance into the cavity. From the Nernst equation the equilibrium potentials of the hydrogen and copper reactions decrease and increase, respectively, with increasing x. Thus, the possibility of overlap of the two electrode potential regions decreases, rather than increases, with increasing distance into the cavity as illustrated in Fig. 9. Similarly, for cathodic polarization of the Cu-Au alloy (Fig. 8), the pH increases which again produces a shift of the equilibrium potential for the h.e.r. in the negative potential direction. As some Cu^{2+} ions initially form by dissolution (since the bulk solution had none), their concentration also increases with distance into the cavity under the influence of the solution potential which decreases with increasing x (3), in which case the copper equilibrium potential becomes more positive with increasing distance into the cavity, i.e., the same situation as for anodic polarization shown in Fig. 9. Thus, for both anodic and cathodic polarization of noble metal alloys in strong acids the equilibrium potentials of the h.e.r. and of the metal dissolution reaction at the crack tip will always be further apart. Since for non complexing solutions there is no overlap at the outer surface it follows that for either polarization mode there is no value of the electrode potential which would allow both the h.e.r. and metal dissolution to occur at the crack tip.

Thus, the solutions to the questions of overlap and cracking mode were easily obtained and it was not even necessary to determine the actual concentrations in the cavity. Had one or more of the concentrations changed in the opposite direction with increase in x it would have been necessary, at least, to estimate the actual concentration values within the cavity. To this end the mathematical model for cathodic polarization (3) is more suited because the total concentration decreases with distance into the cavity, in contrast to an increase for anodic polarization. Thus, the assumption of non-interaction among ionic species in the model is more fully realized for cathodic polarization. In addition, these models assume only soluble reaction products. The quality of the calculation sharply decreases as gas bubbles or solid corrosion products occupy the cavity volume. Evenso, the treads in Figs. 7 and 8 are well established, in which case overlap of the h.e.r. and copper dissolution reactions is not to be expected (in the noble metal alloys).

Stress Corrosion or Hydrogen Cracking in Noble Metal Alloys

The above analysis shows that for noble metal alloys the crack tip electrode potential will not be in the potential region of the alternative reaction, i.e., for anodic polarization the electrode potential in the cavity will not be in the potential region of the h.e.r., and visa versa. This is illustrated in Fig. 9 and is most simply the result of the fact that the E_{LIM} values of the two reactions do not lie in each others potential region.

It follows that crack propagation during anodic polarization is not due to hydrogen and during cathodic polarization is not due to anodic metal dissolution. Table 2 lists known cases of cracking in noble metal alloys which are reexamined based on the above E_{LIM} concept as to whether the fracture process was one of metal dissolution (SCC) or hydrogen cracking (HC). In cases of cracking during open circuit corrosion, Table 2 includes only those cases for which the measured corrosion potential was in the potential region of metal dissolution by virtue of the addition to the electrolyte of a strong oxidant, e.g., HNO_3 or ferric ion, in which case it was clear that the open-circuit condition was equivalent to anodic polarization.

TABLE 2. The mode of cracking (SCC or HC) based on the E_{LIM} criterion for known cases of crack propagation in noble metal alloys for different modes of polarization (11-15).

Alloy	Solution	Mode	SCC or HC
Cu-18a/o Au	H_2SO_4(dil.)	anodic	SCC
	or KCl	anodic	SCC
	or $FeCl_3$	OCP*	SCC
Cu_3Au	$FeCl_3$	OCP	SCC
Cu-25a/o Au	1M H_2SO_4+	OCP	SCC
Cu-40a/o Au	Ce^{4+} ions	OCP	SCC
Ag-20a/o Au	HNO_3	OCP	SCC
	or $FeCl_3$	OCP	SCC
Ag-15a/o Pd	Aqua Regia	OCP	SCC
	or $FeCl_3$		

*OCP (open circuit potential)

Stress Corrosion or Hydrogen Cracking in Other Alloys

For alloys containing base metals the anodic and cathodic polarization curves overlap, and as a result the E_{LIM} values lie in each others potential regions. Let us consider the brass system which has a long history of environmental cracking and continues to be the focus of mechanistic studies in many laboratories. The least noble metal in brass is Zn, and its polarization curve and that of the h.e.r. overlap even at neutral and higher pH. The E_{LIM} values in this case are the mixed potentials established within the crack for the reactant/product concentrations established by the anodic or cathodic polarization processes, Fig. 10.

The (partial) anodic polarization curves for Zn and Cu from -brass in Fig. 10 exhibit characteristic alloy dissolution behavior (16). For anodic polarization of the sample (E_A), the electrode potential within a crevice or crack will range to the left of E_a and can approach E_{LIM} at the most confined region such as a crack tip. As such H(ad) may be formed on the crack-tip surface by reduction of H^+ ion, thereby introducing the possibility of HC in addition to anodic SCC.

Conversely, during cathodic polarization at E_c, the electrode potential inside a crack ranges to the right of E_c towards the mixed potential of the polarization curves (representing different local compositions than for anodic polarization). That part of the crack in the range between $E_{Zn/Zn^{++}}$ and E_{LIM} undergoes preferential dissolution of Zn along with the h.e.r. (at a somewhat reduced rate from that at the outer surface (3)). Hence, both forms of cracking may occur for either cathodic or anodic polarization.

Conclusions

This paper reviews the conditions needed to determine whether aqueous-phase crack propagation occurs due to hydrogen (HC) or due to anodic metal dissolution (SCC). It shows that the main question to be answered is whether overlap of the electrode potential regions of the metal dissolution and hydrogen evolution reactions increases or decreases with increasing distance x into a cavity or crack. It also reviews the theoretical and experimental basis of the recently discovered existence of a limiting electrode potential, E_{LIM}, in a cavity, a finding which is paramount to the goal of this paper. Its findings are:

(1) In acid solutions, overlap of the electrode potential regions of metal dissolution and the h.e.r. decreases with increasing distance x into a cavity. For noble metal alloys in non complexing solutions overlap does not occur at any pH.

(2) Noble metal alloys which are otherwise free of hydrogen can crack by either one, but not both, of the modes depending on the polarization condition: HC during cathodic polarization and SCC during anodic polarization or during open circuit corrosion in the presence of an oxidant.

(3) For base metal alloys the potential regions of metal dissolution and the h.e.r. overlap and, therefore, HC and SCC are both, in principle, possible for either anodic or cathodic polarization.

Acknowledgements

Financial support of the Office of Naval Research under Contract No. N00014-81-K-0025 is gratefully acknowledged.

References

1. H. W. Pickering and R. P. Frankenthal, J. Electrochem. Soc., 119, 1297 (1972).
2. D. Harris and H. W. Pickering, Effect of Hydrogen on the Behavior of Materials, A. W. Thompson, I. M. Bernstein, and A. J. West, ed; pp. 229-231 AIME, Warrendale, PA, (1976).
3. B. G. Ateya and H. W. Pickering, J. Electrochem. Soc., 122, 1028 (1975).
4. H. W. Pickering and A. Valdes, Localized Crack Chemistry and Mechanics in Environment Assisted Cracking, R. P. Gangloff ed., AIME, Warrendale, PA, (1984) to be published.
5. B. G. Ateya and H. W. Pickering, Hydrogen in Metals, I. M. Bernstein and A. W. Thompson, ed; pp. 206-222 ASM, Metals Park, OH (1974).
6. H. W. Pickering, H. H. Uhlig Symposium, Corrosion and Corrosion Protection, R. P. Frankenthal and F. Mansfeld eds., pp. 85-91 The Electrochem. Soc. Inc., Pennington, NJ, (1981).
7. G. Herbsleb and H. J. Engell, Z Electrochem., 65 881 (1961); Werkstoffe und Korrosion, 17, 365 (1966).
8. N. D. Greene, W. D. France, Jr., and B. E. Wilde, Corrosion, 21, 175 (1965).
9. C. M. Chen, F. H. Beck, and M. G. Fontana, Corrosion, 27, 234 (1971).
10. C. B. Bargeron and R. C. Benson, J. Electrochem. Soc., 127, 2528 (1980).
11. H. Gerischer and H. Rickert, Z. Metallkunde, 46, 681 (1955).
12. R. Bakish and W. Robertson, Trans. AIME, 206, 1277 (1956).
13. H. W. Pickering, Corrosion, 25, 289 (1969).
14. L. Graf and J. Budke, Z. Metallkunde, 46, 378 (1955).
15. L. Graf, Fundamental Aspects of Stress Corrosion Cracking, R. W. Staehle, A. J. Forty and D. van Rooyan, eds., pp. 187 to 201, N.A.C.E., Houston, Texas (1969).
16. H. W. Pickering, Corros. Sci., 23, 1107 (1983).

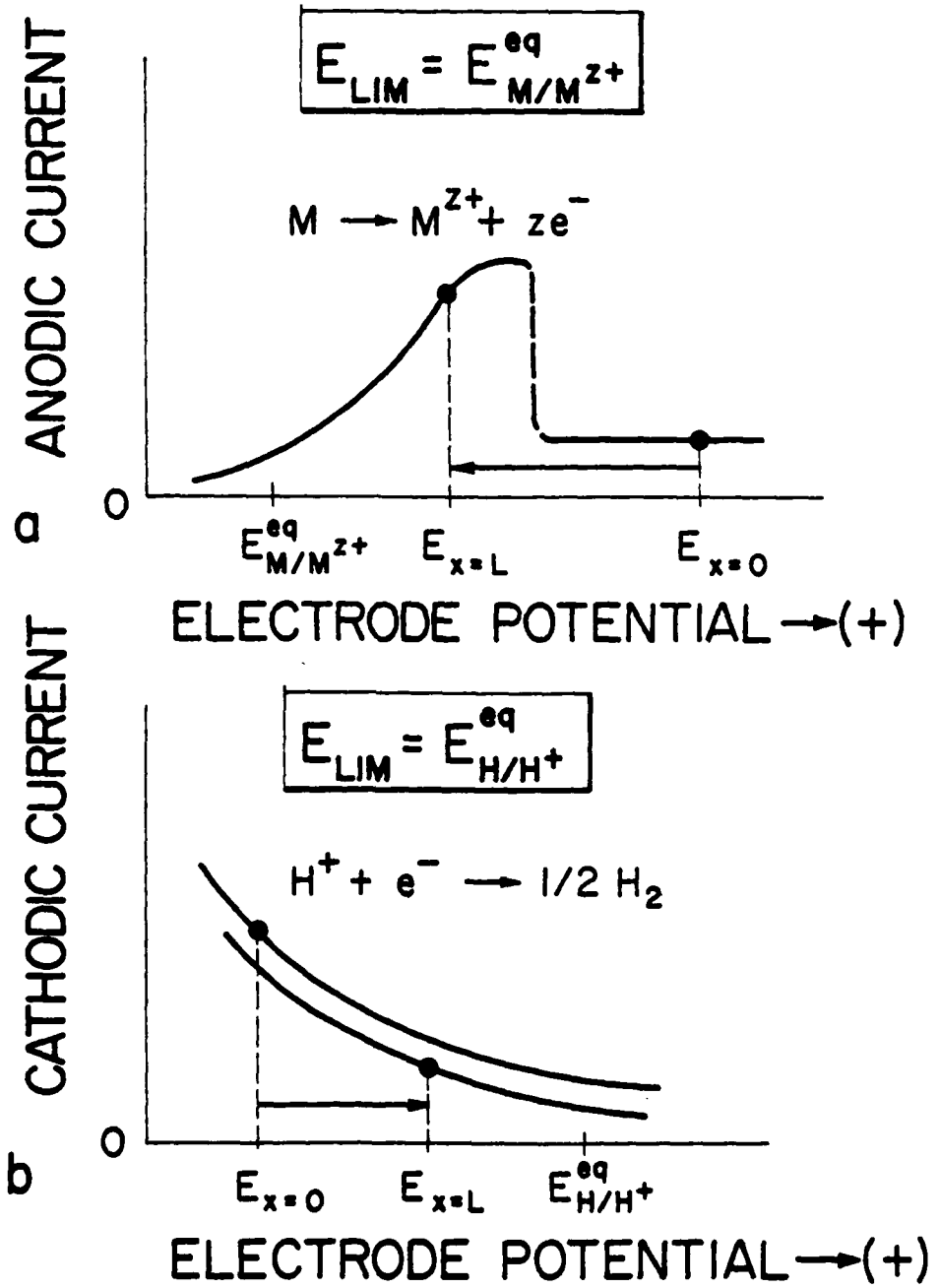

Figure 1. Schematic of the limiting electrode potential and shift of the $E_{x=0}$ value to the $E_{x=L}$ value (a) during pitting or crevice corrosion, and (b) within a crack during hydrogen evolution

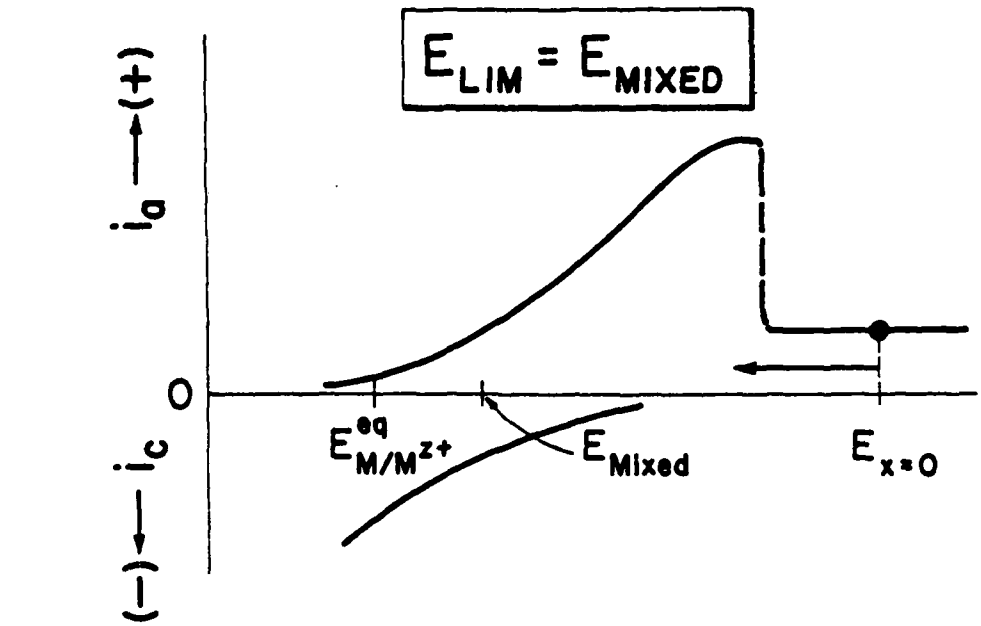

a

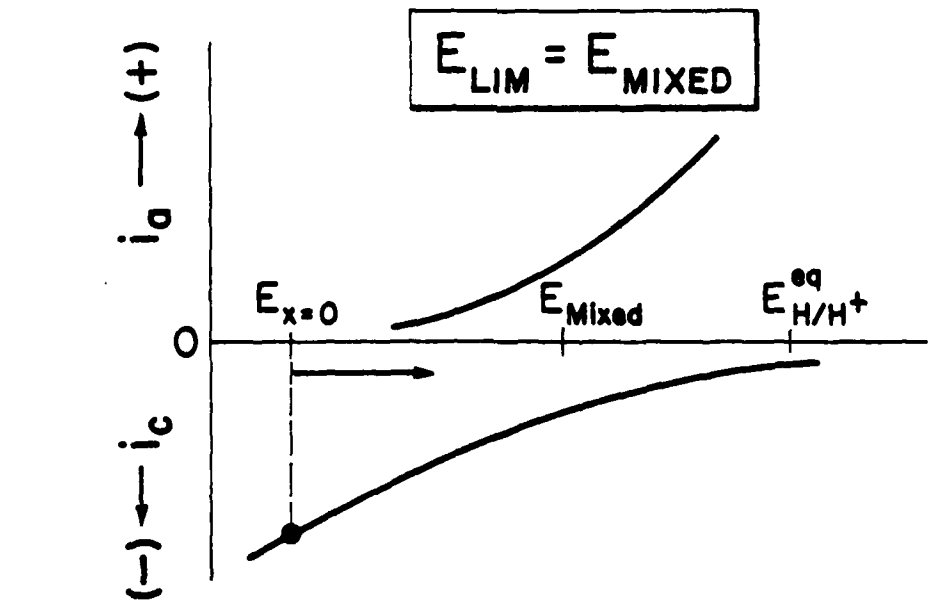

b

Figure 2. As in Figure 1 but illustrating that E_{LIM} is the mixed potential when reactions of opposite sign occur within the cavity.

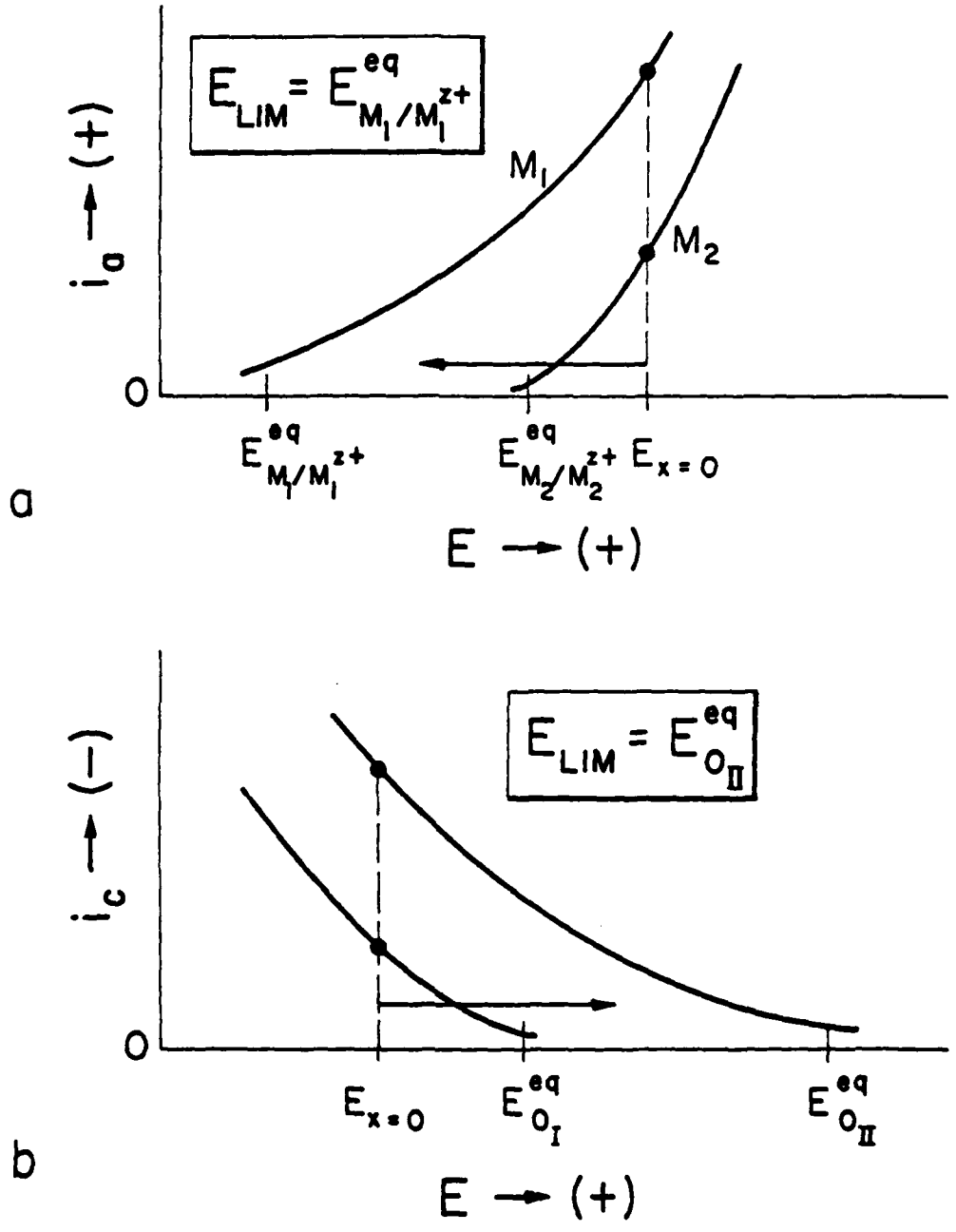

Figure 3. As in Figure 1 but illustrating that E_{LIM} is the equilibrium potential of the most favored reaction of two or more reactions of the same sign in a cavity.

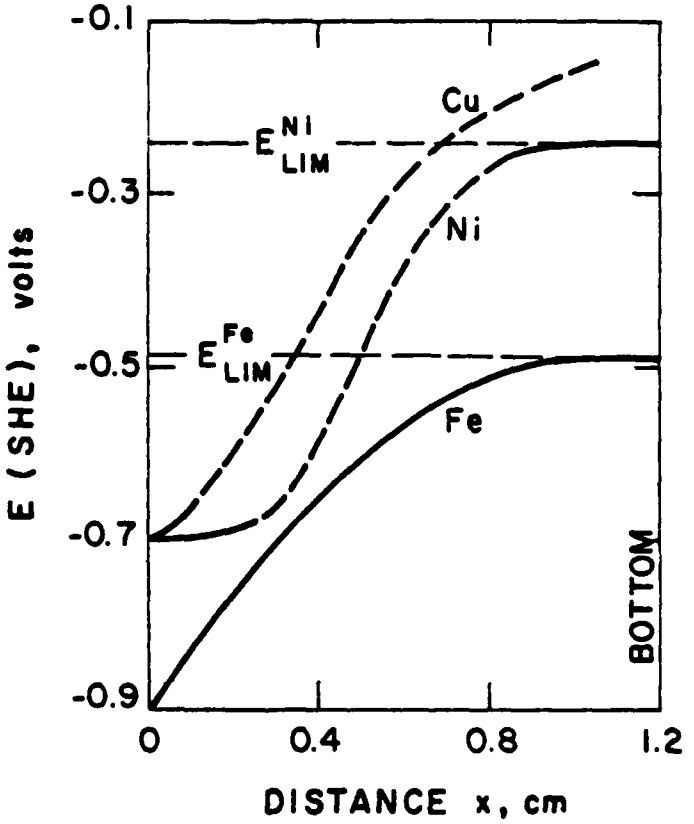

Figure 4. The measured electrode potential profiles inside cavities in samples of Cu, Ni and Fe during cathodic polarization for the conditions in Table 1.

Figure 5. In-place hydrogen gas bubbles which formed during cathodic polarization at 9 A m^{-2}, photographed through a transparent plastic which was used as one wall of the crevice. The other wall and top surface were the iron sample (2).

Figure 6. SEM micrograph illustrates etching of the iron at the point of contact of the largest in-place bubble in Figure 5 (2).

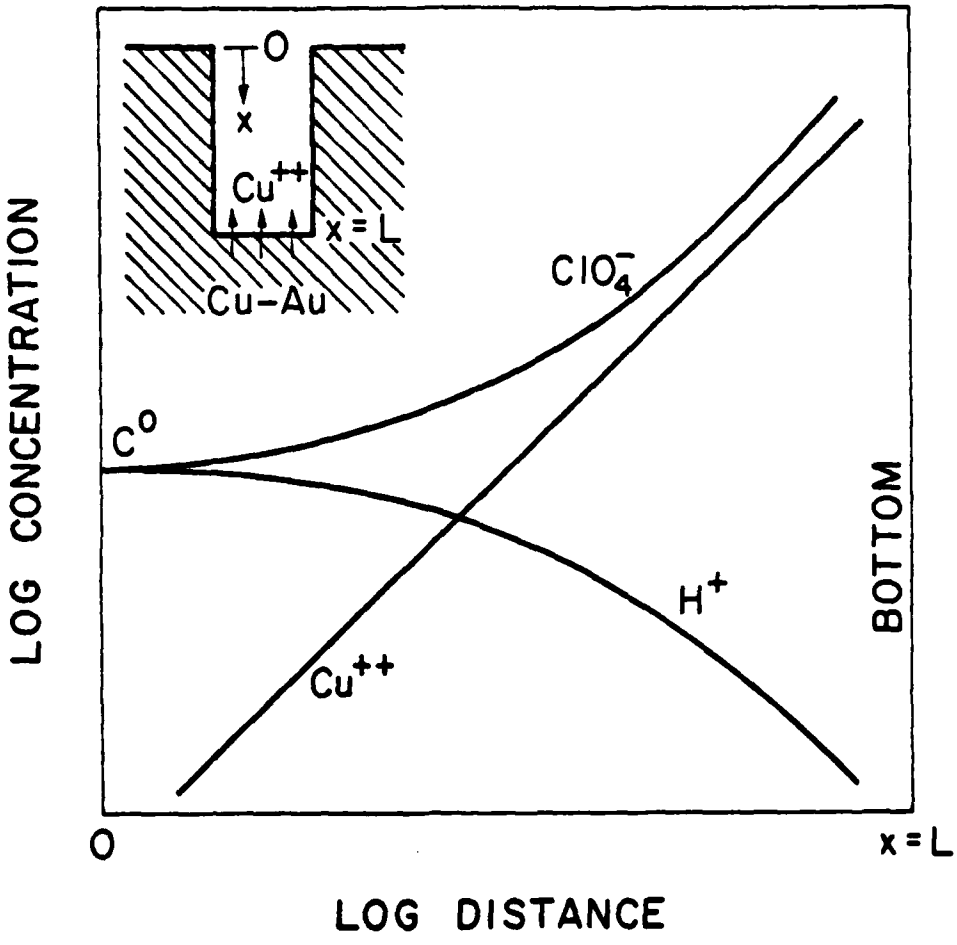

Figure 7. Concentration profiles within $HClO_4$ acid in a pit in Cu-Au alloy. Model is for a single reaction, steady state Cu dissolution within a pit (1). At the outer surface Cu dissolution is a assumed to be negligible in accord with experimental results which show that Au blocks the Cu dissolution reaction (11).

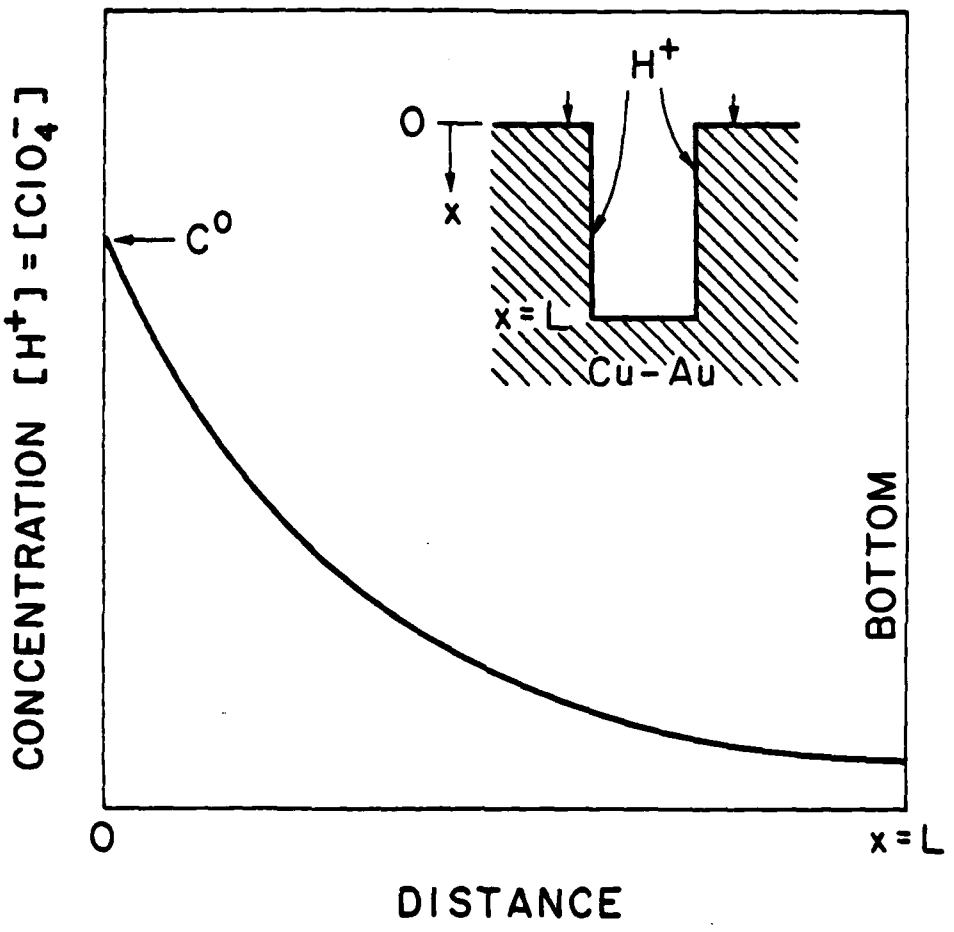

Figure 8. Concentration profiles for cathodic polarization of the system in Figure 7. Model is for a single reaction (h.e.r.) occurring within the cavity as well as on the outer surface (3).

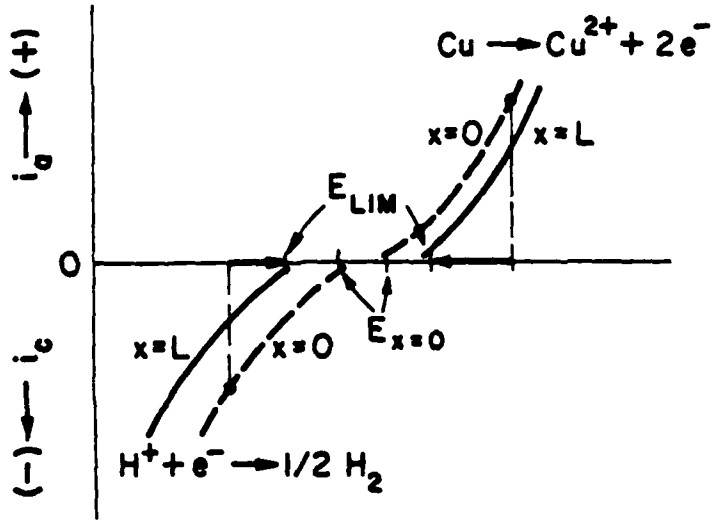

Figure 9. Schematic illustrating an increased separation of $E^{eq}_{M/M^{z+}}$ and $E^{eq}_{H/H^{+}}$ with increasing distance x into the cavity and, therefore, no chance of overlap of their respective polarization curves.

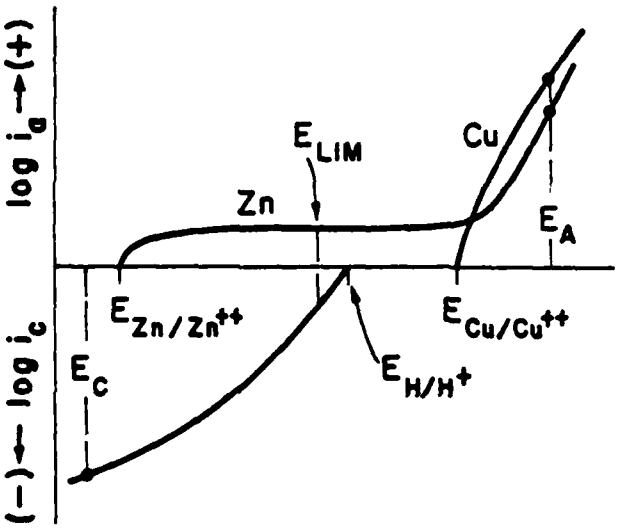

Figure 10. Schematic illustrating that E_{LIM} for brass and other alloys containing a base metal is in the region of the h.e.r.

BASIC DISTRIBUTION LIST

Technical and Summary Reports November 1979

Organization	Copies
Defense Documentation Center Cameron Station Alexandria, VA 22314	12
Office of Naval Research Department of the Navy 800 N. Quincy Street Arlington, VA 22217 ATTN: Code 471 Code 470	1 1
Commanding Officer Office of Naval Research Branch Office Building 114, Section D 666 Summer Street Boston, MA 02210	1
Commanding Officer Office of Naval Research Branch Office 536 South Clark Street Chicago, IL 60605	1
Naval Research Laboratory Washington, DC 20375 ATTN: Codes 6000 6100 6300 2627	1 1 1 1
Naval Air Development Center Code 606 Warminster, PA 18974 ATTN: Dr. J. Deluccia	1
Naval Air Propulsion Test Center Trenton, NJ 08628 ATTN: Library	1
Naval Construction Batallion Civil Engineering Laboratory Port Hueneme, CA 93043 ATTN: Materials Division	1
Naval Electronics Laboratory San Diego, CA 92152 ATTN: Electron Materials Sciences Division	1
Naval Missile Center Materials Consultant Code 3312-1 Point Mugu, CA 92041	1
Commanding Officer Naval Surface Weapons Center White Oak Laboratory Silver Spring, MD 20910 ATTN: Library	1
Commander David W. Taylor Naval Ship Research and Development Center Bethesda, MD 20084	1
Naval Oceans Systems Center San Diego, CA 92132 ATTN: Library	1
Naval Underwater System Center Newport, RI 02840 ATTN: Library	1
Naval Postgraduate School Monterey, CA 93940 ATTN: Mechanical Engineering Department	1
Naval Weapons Center China Lake, CA 93555 ATTN: Library	1

BASIC DISTRIBUTION LIST (cont'd)

Organization	Copies
Naval Air Systems Command Washington, DC 20360 ATTN: Codes 52031	1
52032	1
Naval Sea System Command Washington, DC 20362 ATTN: Code 05R	1
Naval Facilities Engineering Command Alexandria, VA 22331 ATTN: Code 03	1
Scientific Advisor Commandant of the Marine Corps Washington, DC 20380 ATTN: Code AX	1
Army Research Office P.O. Box 12211 Triangle Park, NC 27709 ATTN: Metallurgy & Ceramics Program	1
Army Materials and Mechanics Research Center Watertown, MA 02172 ATTN: Research Programs Office	1
Air Force Office of Scientific Research/NE Building 410 Bolling Air Force Base Washington, DC 20332 ATTN: Chemical Science Directorate	1
Electronics & Materials Sciences Directorate	1
AFWAL/MLL Wright-Patterson AFB Dayton, OH 45433	1
Library Building 50, Room 134 Lawrence Radiation Laboratory Berkeley, CA 94700	1
NASA Headquarters Washington, DC 20546 ATTN: Code RRM	1

Organization	Copies
NASA Lewis Research Center Lewis Research Center 21000 Brookpark Road Cleveland, OH 44135 ATTN: Library	1
National Bureau of Standards Washington, DC 20234 ATTN: Metals Science and Standards Division	1
Ceramics Glass and Solid State Science Division	1
Fracture and Deformation Division	1
Director Applied Physics Laboratory University of Washington 1013 Northeast Forthieth Street Seattle, WA 98105	1
Defense Metals and Ceramics Information Center Battelle Memorial Institute 505 King Avenue Columbus, OH 43201	1
Metals and Ceramics Divison Oak Ridge National Laboratory P.O. Box X Oak Ridge, TN 37380	1
Los Alamos Scientific Laboratory P.O. Box 1663 Los Alamos, NM 87544 ATTN: Report Librarian	1
Argonne National Laboratory Metallurgy Division P.O. Box 229 Lemont, IL 60439	1
Brookhaven National Laboratory Technical Information Division Upton, Long Island New York 11973 ATTTN: Research Library	1
Office of Naval Research Branch Office 1030 East Green Street Pasadena, CA 91106	1

Sept 1980

SUPPLEMENTARY DISTRIBUTION LIST

Technical and Summary Reports

Dr. T. R. Beck
Electrochemical Technology Corporation
31st Avenue, NE
Seattle, Washington 98125

Professor I. M. Bernstein
Carnegie-Mellon University
Schenley Park
Pittsburgh, Pennsylvania 15213

Professor H. K. Birnbaum
University of Illinois
Department of Metallurgy
Urbania, Illinois 61801

Dr. Otto Buck
Rockwell International
1049 Camino Dos Rios
P.O. Box 1085
Thousand Oaks, California 91360

Dr. W. Morris
Rockwell International
1049 Camino Dos Rios
P.O. Box 1085
Thousand Oaks, California 91360

Dr. David L. Davidson
Southwest Research Institute
8500 Culebra Road
P.O. Drawer 28510
San Antonio, Texas 78284

Dr. D. J. Duquette
Department of Metallurgical Engineering
Rennsselaer Polytechnic Institute
Troy, New York 12181

Professor R. T. Foley
The American University
Department of Chemistry
Washington, D. C. 20016

Dr. J. A. S. Green
Martin Marietta Corporation
1450 South Rolling Road
Baltimore, Maryland 21227

Professor R. H. Heidersbach
University of Rhode Island
Department of Ocean Engineering
Kingston, Rhode Island 02881

Professor H. Herman
State University of New York
Material Sciences Division
Stony Brook, New York 11790

Professor J. P. Hirth
Ohio State University
Metallurgical Engineering
1314 Kinnear Road
Columbus, Ohio 43212

Professor R. M. Latanision
Massachusetts Institute of Technology
77 Massachusetts Avenue
Room E19-702
Cambridge, Massachusetts 02139

Dr. F. Mansfeld
Rockwell International Science Center
1049 Camino Dos Rios
P.O. Box 1085
Thousand Oaks, California 91360

Dr. Jeff Perkins
Naval Postgraduate School
Monterey, California 93940

Dr. E. A. Starke, Jr.
Georgia Institute of Technology
School of Chemical Engineering
Atlanta, Georgia 30332

Dr. R. P. Wei
Lehigh University
Institute for Fracture and
Solid Mechanics
Bethlehem, PA 18015

SUPPLEMENTARY DISTRIBUTION LIST (continued)

Professor H. C. F. Wilsdorf
University of Virginia
Department of Materials Science
Charlottesville, Virginia 22903

Dr. Clive Clayton
State University of New York
Material Sciences Division
Stony Brook, New York 11970

Dr. Henry Leidheiser
Center for Surface and Coatings Research
Sinclair Memorial Laboratory 7
Lehigh University
Bethlehem, PA 18015

Prof. Morris E. Fine
Northwestern University
The Technological Institute
Evanston, IL 60201

Dr. C. S. Kortovich
TRW, Inc.
2355 Euclid Avenue
Cleveland, OH 44117

Dr. J. Kruger
National Bureau of Standards
Washington, DC 20234

Dr. Barry C. Syrett
Stanford Research Institute
333 Ravenswood Avenue
Menlo Park, CA 94025

Prof. S. Weissmann
Rutgers, The State University
of New Jersey
College of Engineering
New Brunswick, NJ 08903

Dr. R. J. Arsenault
University of Maryland
College Park, MD 20742

Prof. A. J. Ardell
University of California
School of Engineering & Applied Science
405 Hilgard Ave.
Los Angeles, CA 90024

Prof. J. G. Byrne
The University of Utah
Dept. of Materials Science & Engineering
Salt Lak City, Utah 84112

Prof. Alexander M. Cruickshank
Gordon Research Conference
Pastore Chemical Laboratory
University of Rhode Island
Kingston, RI 02881

Dr. Paul Gordon
Illinois Institute of Technology
Department of Metallurgical and Materials
Engineering
Chicago, IL 60616

Dr. J. V. McArdell
University of Maryland
College Park, MD 20742

Dr. E. McCafferty
Naval Research Laboratory
Washington, DC 20375

Prof. G. H. Meier & F. S. Pettit
University of Pittsburgh
Dept. of Metallurgical and Materials
Engineering
Pittsburgh, PA 15261